Dynamic Equilibrium in Histone Assembly: Self-Assembly of Single Histones and Histone Pairs†

Ruth Sperling* and Michael Bustin

ABSTRACT: The assembly of acid-extracted, purified F_2a_1, F_3, F_2a_2, and F_2b histones and their six possible pairwise combination into organized structures has been studied by: (1) sedimentation velocity, (2) sedimentation equilibrium, (3) electrophoresis in polyacrylamide gels containing sodium dodecyl sulfate after cross-linking the protein solutions with dimethyl suberimidate, and (4) electron microscopy. Each of the purified histone fractions can renature and assemble into high molecular weight organized structures. This assembly is dependent on the ionic strength, protein concentration, and temperature of the solutions. The four histones studied assemble into structures of similar dimensions and shape. In each case the first structure observed is a bent rod with a diameter of 22 Å. Conditions which favor assembly lead to formation of fibers with diameters of about 44 Å. The conditions which lead to assembly into organized structures are similar for the arginine-rich histones, F_2a_1 and F_3. Higher ionic strength is required for the assembly of the lysine-rich histones, F_2a_2 and F_2b. Certain pairs of histones interact. Strong interactions among pairs of histones interfere with the self-assembly of single histones into large structures. However, increase in protein concentration or ionic strength leads to formation of large molecular structures even in solutions of pairs of strongly interacting histones. These structures are similar to those obtained with single histones. The results suggest that aggregation and complexing of histones represent a reversible, ordered process of assembly. The various assembled forms are in a dynamic equilibrium. The final assembled form, which is similar in all cases, is dependent on the environmental conditions to which the histones are exposed. It is suggested that each of the assembled histone structures, regardless whether it is composed of a single histone or a pair of histones, can serve as a core around which the DNA can be wrapped.

It is a long standing observation that histones at neutral pH and moderate salt concentrations aggregate (Hnilica, 1972). This aggregation which is observable by a variety of techniques led to the erroneous conclusion that the histones are a highly heterogeneous class of basic proteins (Hnilica, 1972). Presently it is recognized that the histones found in most eukaryotes can be resolved into five major types of histones (Hnilica, 1972). Some of the properties which may be pertinent to their structural role and which are common to all histones are: (1) the histones exhibit little qualitative and quantitative specificity and their primary sequence is highly conserved, (2) the distribution of amino acids along the histone polypeptide chain is such that basic residues and hydrophobic residues tend to cluster, thereby giving rise to regions of high cationic charge and low hydrophobicity, and (3) the conformation of histones is highly affected by a variety of conditions such as pH, ionic strength, temperature, and protein concentration.

An increase in ionic strength or pH generally raises the percentage of α helix in the molecule (Hnilica, 1972). In some cases this α-helix formation is followed by β-sheet formation and aggregation (Li et al., 1972). Bradbury and his coworkers (Bradbury et al., 1973) have used nuclear magnetic resonance (NMR) techniques to identify the segments of the histone molecules that undergo the most pronounced conformational changes upon addition of salt. Isenberg and his associates have used circular dichroism, light scattering, and fluorescence anisotropy to show that salt induces conformational changes and aggregation in histones (D'Anna and Isenberg, 1972, 1973; Wickett et al., 1972; Smerdon and Isenberg, 1973). We have demonstrated that the arginine-rich histone F_2a_1 reversibly assembles into organized periodic structures visualized by electron microscopy (Sperling and Bustin, 1974).

Recent studies point out that pairs of histones interact with each other to form well-defined complexes. Thus, D'Anna and Isenberg reported that histones F_2a_1 and F_2b (1973) and histones F_2b and F_2a_2 (1974b) interact at 1:1 molar ratios to form strong complexes with association constants of $10^6\ M^{-1}$. Similarly F_2a_1 and F_3 interact with an association constant of $0.7 \times 10^{21}\ M^{-3}$, calculated for a tetramer (D'Anna and Isenberg, 1974c). Other histone pairs form weaker complexes (D'Anna and Isenberg, 1974c). Skandrani et al. (1972) and Kelley (1973) isolated and characterized an F_2b and F_2a_2 complex. This complex was also observed by Kornberg and Thomas (1974) who studied the complexing of histones extracted by the salt procedure of van der Westhuyzen and von Holt (1971). This salt procedure also yields an F_2a_1·F_3 complex which was found to be a tetramer by Kornberg and Thomas (1974) and a dimer in equilibrium with a tetramer by Roark et al. (1974). D'Anna and Isenberg (1974d) obtained this tetramer from acid-extracted histones.

It seems therefore that single histone species can either self-assemble into relatively large well-defined structures or complex with each other to give heterocomplexes. The various reassembled structures may be in a dynamic equilibrium and the final structure obtained will be determined by the exact conditions to which the histones are exposed. The aim of the present investigation was to study this equilibrium, characterize the structures formed, and define parame-

†From the Departments of Chemical Physics and Chemical Immunology, Weizmann Institute of Science, Rehovot, Israel. *Received February 18, 1975.* This work was supported by grants from the Israel Commission for Basic Research.

ters which lead to their formation. In this study, acid-extracted, purified histones have been used.

The tertiary structure of a protein is determined by its primary structure (Anfinsen, 1973). In an assembly system the quaternary structure is affected by the tertiary structure of the components. However, in an assembly system several structures, which have a local minimum in their free energy, may exist. Thus the formation of a specific structure may depend on the specific environmental conditions of the preparation. Kinetic as well as thermodynamic factors may affect the final structure obtained.

In view of this, we have prepared histone pairs by first equilibrating each one in low salt and allowing sufficient time for dissociation to low molecular weight structures. The pairs are then mixed at low salt and given sufficient time to interact. Finally, the salt concentration is increased by dialysis. The effect of protein concentration, ionic strength, and temperature on the assembly of single histones and on the assembly of pairs of histones has been studied. This assembly has been studied by sedimentation velocity and sedimentation equilibrium, by electron microscopy, and by electrophoresis in sodium dodecyl sulfate containing gels after cross-linking with dimethyl suberimidate (Davies and Stark, 1970).

Materials and Methods

Histones. Calf thymus was obtained from a local slaughterhouse and transported to the laboratory on ice. Histones were extracted from the washed nucleoprotein with H_2SO_4 and fractionated on Bio-Gel P60 equilibrated and eluted with 0.02 *M* HCl, 0.1 *M* NaCl, and 0.02% NaN_3 (Bohm et al., 1973). F_2a_2 and F_3 were separated by affinity chromatography (Ruiz-Carrillo and Allfrey, 1973). Where necessary, histones were further purified by filtration through Sephadex G-100 or chromatography on IRC-50 (Luck et al., 1958). The final purity of the samples was judged by the electrophoretic pattern in polyacrylamide gels (Panyim and Chalkley, 1969).

Preparation of Histone Solutions. Lyophilized histones were dissolved in 10 m*M* HCl solutions. The concentrations of the solutions were determined by measuring the absorbance at 278 nm. The optical densities of 1-mg/ml histone solutions were taken to be 0.50, 0.45, 0.36, and 0.28 for F_2b, F_2a_1, F_2a_2, and F_3 respectively (Johns, 1971). The solutions (except F_3) were then dialyzed extensively at 5°, in boiled dialysis bags, against sodium cacodylate buffer (pH 7.0), I = 0.01. After this stage the solution was brought to the desired ionic strength by dialysis against NaCl containing solutions. The solutions were left to equilibrate at each ionic strength for at least 12 hr prior to examination. All the solutions containing F_3 were prepared by making the solutions 0.01 *M* in β-mercaptoethanol and dialyzing against salt solution containing 1×10^{-4} β-mercaptoethanol.

To prepare histone pairs, the single histones in cacodylate buffer (pH 7.0), I = 0.01, 5°, were mixed in equimolar ratios. The pairs were kept at these conditions for at least 4 hr before increasing the ionic strength of solutions. All pairs containing F_3 were dialyzed against solutions containing 1×10^{-4} *M* β-mercaptoethanol. Solutions examined at 20° were prepared at 5° as described above, and were left to equilibrate at 20° for 12 hr prior to examination.

Electron Microscopy. A drop of the specimen solution was placed upon a carbon-coated grid and washed with a few drops of buffer and then with a few drops of 1% solution of uranyl acetate. The excess liquid was withdrawn with the edge of a filter paper. A Phillips EM 300 electron microscope operated at 80 kV was used.

Ultracentrifugation. Sedimentation velocity measurements at 5 and 20° were run at 44,000 and 56,000 rpm in a Beckman Model E analytical ultracentrifuge equipped with photoelectric speed control using a double or single sector capillary type synthetic boundary cell. Equilibrium sedimentations were run in the same instrument equipped with a uv scanner. Runs were made at 5° and at speeds of 12,000 rpm using an AN-J rotor. A value of 0.74 $cm^3\ g^{-1}$ was used for $\bar{V}$, the partial specific volume.

Cross-Linking and Electrophoresis in Polyacrylamide Gels. Histone solutions at various protein concentrations were cross-linked at pH 8.0, with dimethyl suberimidate (Davies and Stark, 1970). For cross-linking, solutions of 20.0 mg/ml of dimethyl suberimidate were prepared just prior to reaction; 100 μl of such solutions was added to 0.25-ml histone solutions to give a molar ratio of cross-linker/histone of 100–300:1. The reaction was stopped by adding an excess of D,L-lysine and dialyzing against cacodylate buffer (pH 7.0). After dialysis the solutions were made 0.1% in sodium dodecyl sulfate, heated for 2 hr at 37° and electrophoresed on either 4, 7.5, or 10% polyacrylamide gels (Weber and Osborn, 1969). The gels were calibrated with known markers. Gels were scanned with a Gilford linear transport gel scanner. In some cases the cross-linking reaction was stopped by addition of HCl. Glutaraldehyde was also used as cross-linker. The exact procedure used in each case is described in legends to figures.

Results and Discussion

I. Self-Assembly of Single Histones

Sedimentation. Solutions of histones at a concentration of 1.0 mg/ml in cacodylate buffer (I = 0.01) and sodium chloride (I = 0.15) (pH 7.0) at 5 and 20° were subjected to sedimentation velocity measurements. The results obtained at 5° are presented in Figure 1. Under these conditions, F_2a_2 displayed a single peak (95% of the material) with an $s_{20,w}$ of 2.4 S. The other three histones displayed two major fractions, a low molecular weight and a high molecular weight fraction. In the case of the arginine-rich histones, F_2a_1 and F_3, over 50% of the material was in the high molecular weight fraction, while in the case of histone F_2b, 80% of the material was in the low molecular weight fraction.

The relative amounts of the low and high molecular weight fractions are dependent on the environmental conditions. When the temperature was elevated to 20° the relative amount of the higher molecular weight component increased to 90% with F_2a_1 and to 80% for F_3. For F_2b and F_2a_2, however, no significant temperature effect was observed. Upon raising the protein concentration the proportion of the high molecular weight component increased in all histone fractions.

The ionic strength had a similar effect on the equilibrium. The results obtained by elevating the ionic strength to I = 0.3 are summarized in Table I. It can be seen that for each histone species an increase in ionic strength brought about a rise in the percentage of the high molecular weight fraction ($s_{20,w}$ >6). This effect was most dramatic for the slightly lysine-rich histones F_2a_2 and F_2b. The arginine-rich histones F_2a_1 and F_3 had a high fraction of fast sedimenting material already at I = 0.15.

These findings suggest that purified histone fractions

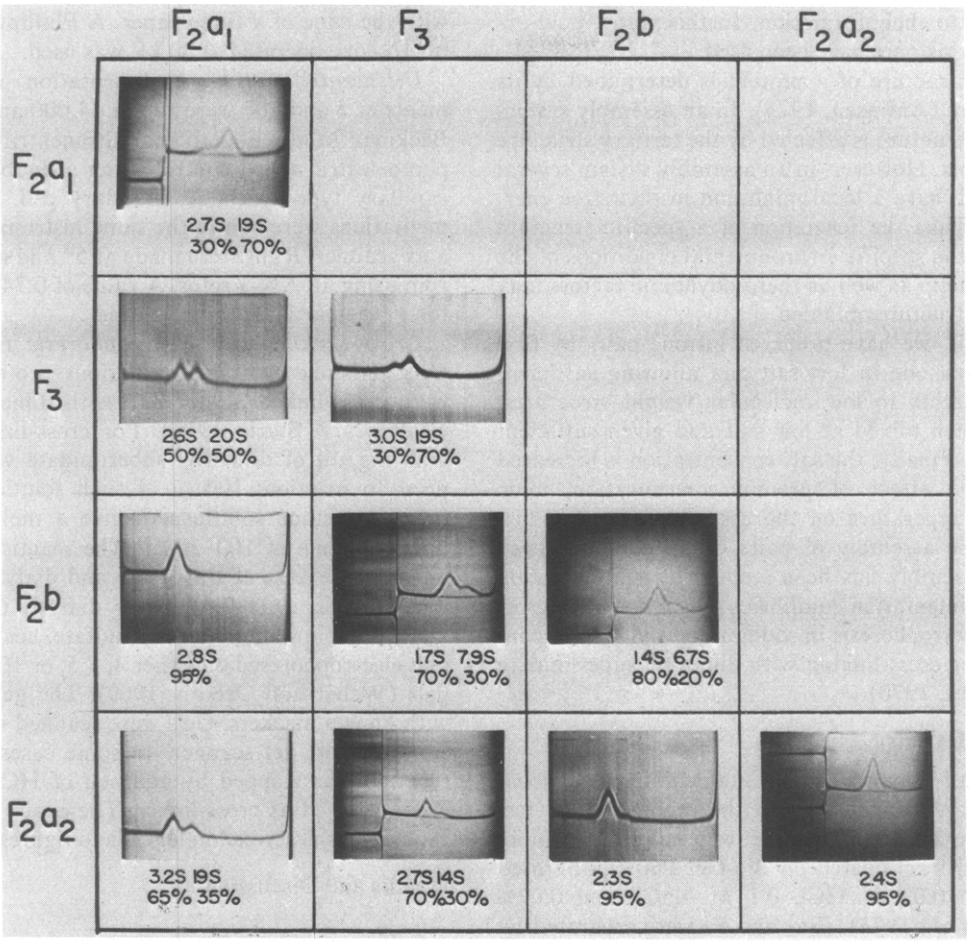

FIGURE 1: Matrix of the self and pairwise interaction of histones F_2a_1, F_3, F_2b, and F_2a_2. Sedimentation patterns of single (1 mg/ml) or pairs of histone at 2.0 mg/ml of protein, in sodium cacodylate buffer (I = 0.01) (pH 7), I = 0.15 (NaCl), 5° (subjected to sedimentation velocity runs as described under Materials and Methods). The single histone species lie on the diagonal of the matrix. The schlieren patterns shown were taken at early times to represent the relative amounts of the high and low molecular weight fractions. (The two fractions completely separated during the course of the run.)

tend to self-assemble into higher molecular weight components. The observation that the relative amounts of the fractions are dependent on the environmental conditions suggests that there is an equilibrium between the low and high molecular weight fractions.

Electron Microscopy. The self-assembly of histones into well-defined organized structures can be observed by electron microscopy. We have previously described the "bent rod" form and the intertwined fibers resulting from the self-assembly of histone F_2a_1 (Sperling and Bustin, 1974). The electron micrographs presented in Figure 2 indicate that similar structures are obtained with other histone fractions. The best defined structures, similar to those described for F_2a_1, are obtained with F_3. With this histone, some bent rods (Sperling and Bustin, 1974) were observed already at ionic strength of 0.01 (Figure 2A). At I = 0.3 intertwined fibers were observed which become more pronounced at I = 0.5 (Figure 2B). The bent rods have an average diameter of 22 Å while the average diameter of the intertwined fibers is 44 Å. The slightly lysine-rich histone F_2b at I = 0.15 displayed a very small amount of bent rods (Figure 2C). The amount of organized structures in this histone increased when the ionic strength was raised to I = 0.3 (Figure 2D). With histone F_2a_2 bent rods were observed only at I = 0.5 (Figure 2E). The assembly into organized structures is promoted by the presence of phosphate ions in the solutions. Thus at 5×10^{-3} M sodium phosphate (pH 7.0) bent rods were observed in solutions of F_2b and F_2a_1 without the addition of NaCl.

Electrophoresis. To estimate the number of subunits in the bent rod form, F_2a_1 histone, at I = 0.15 and 5°, has been subjected to sedimentation equilibrium studies. At protein concentrations ranging between 0.1 and 0.5 mg/ml, Map[1] ranged from 1×10^5 to 5×10^5. To further characterize the major species present, we have cross-linked the single histones with glutaraldehyde or dimethyl suberimidate and analyzed the reaction products by electrophoresis on polyacrylamide gels run in the presence of sodium dodecyl sulfate. However, as there is an equilibrium between the low and high molecular weight fractions the cross-linking may shift the equilibrium toward the high molecular weight fraction. Indeed it was observed that increase in protein concentration or in the duration of cross-linking favored the formation of high molecular weight components. An example of such a situation is presented in Figure 3. When histone F_2a_1 at I = 0.15, 0.1 mg/ml, was cross-linked for 1 hr, a series of bands ranging from monomer up to octamer was clearly distinguishable. The major species was the dimer and no material appeared on top of the gel (solid line, Figure 3A). Since the Map of the protein at 0.1 mg/ml

[1] Abbreviation used is: Map, apparent weight average molecular weight. Obtained by taking the gradient at any point in the plot of ln C vs. r^2, where C is the concentration at r cm from the center of rotation.

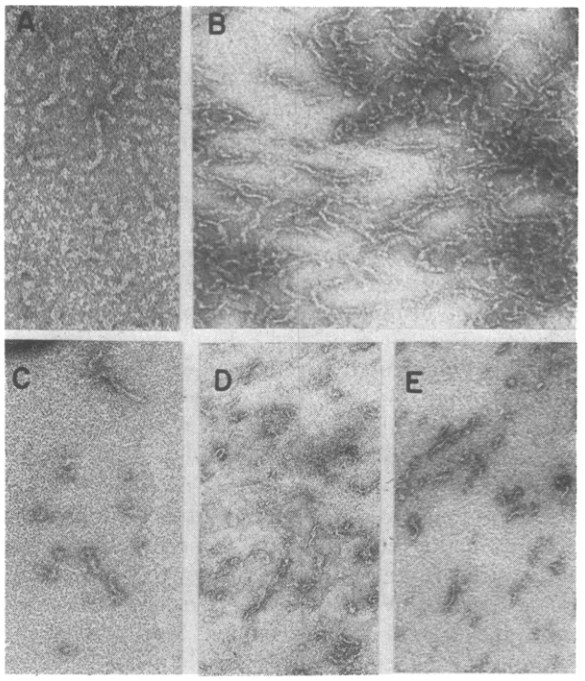

FIGURE 2: Self-assembly of histones: F_3, F_2b, and F_2a_2. Electron micrographs of single histones at 2 mg/ml of protein in sodium cacodylate buffer (pH 7.0) (I = 0.01), 5°, at various ionic strengths (NaCl). (A) F_3 at I = 0.01, ×134,000; (B) F_3 at I = 0.5, ×144,000; (C) F_2b at I = 0.15, ×88,000; (D) F_2b at I = 0.3; ×112,000; (E) F_2a_2 at I = 0.5, ×112,000. B, D, and E were photographed over holes in the carbon-coated grid.

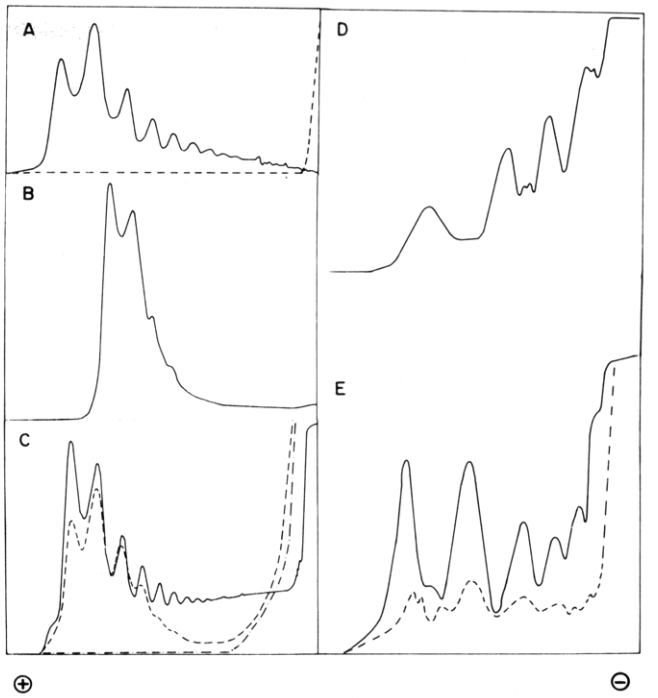

FIGURE 3: Cross-linking of single histone species. (A) F_2a_1 at 0.1 mg/ml, I = 0.15, cross-linked with dimethyl suberimidate. (—) 1 hr cross-linked; (- - -), 4 hr cross-linked. (B) F_2a_1 at 0.5 mg/ml at I = 0.15 cross-linked with dimethyl suberimidate for 15 min (stopped with HCl). (C) F_2a_1 at 0.5 mg/ml, I = 0.15, cross-linked (—) 1 hr with dimethyl suberimidate, (- - - -) 3 hr with dimethyl suberimidate, (- - -) 1 hr with glutaraldehyde. (D) F_2a_2 at 1.0 mg/ml, I = 0.15, cross-linked with dimethyl suberimidate for 1 hr. (E) F_2b at 1.0 mg/ml, I = 0.15, cross-linked with dimethyl suberimidate for (—) 1 hr; for (- - - -) 16 hr. A–C, electrophoresis in 4% polyacrylamide gels; D and E, electrophoresis in 7.5% gels. In each case the peak running fastest to the cathode represents the monomer species. Gels were calibrated with known markers.

Table I: Effect of Ionic Strength on the Assembly of Single Histone Species [a] as Measured by Sedimentation Velocity.

Histone	Component	$s_{20,w}$ I = 0.15	$s_{20,w}$ I = 0.30
F_2a_1	Slow	2.7 (30%)	2.7 (30%)
	Fast	19.0 (70%)	19 (50%); 23–53 (20%)
F_3	Slow	2.6 (50%)	3.0 (30%)
	Fast	20.0 (50%)	20.0 (70%)
F_2b	Slow	1.4 (80%)	3.5 (50%)
	Fast	6.7 (20%)	6 (15%); 9 (15%); 12 (15%)
F_2a_2	Slow	2.4 (95%)	2.4 (45%)
	Fast		8.4 (55%)

[a] Data refer to solutions of 1.0 mg/ml of histones in sodium cacodylate buffer (I = 0.01), pH 7.0, 5°. The ionic strengths were adjusted with NaCl. Percentage values in parentheses refer to amount of particular component.

was 120,000 the cross-linking time was not sufficient to fix the major species present. When the cross-linking time was 4 hr, the equilibrium was shifted toward the high molecular weight form and all the material appeared at the top of the gel (dashed line, Figure 3A).

Similar results were observed at 0.5 mg/ml of protein. When cross-linked for 15 min mostly monomers and dimers accompanied by trimers and tetramers were observed (Figure 3B). After 60 min of cross-linking a series of bands ranging from monomer to octamer together with a high molecular weight band at the top of the gel were observed (see solid line, Figure 3C). Cross-linking for a longer time resulted in the gradual disappearance of the lower bands. After 3 hr of cross-linking all the material was at the top of the gel (dotted line, Figure 3C). When F_2a_1, 0.5 mg/ml, was cross-linked with glutaraldehyde (0.5%, 30 min) a slightly different picture emerged. About 50% of the material gave four bands ranging from monomer to tetramer and the rest was at the top of the gel corresponding to high molecular weight material (dashed line, Figure 3C). The discrepancy between these two cross-linking reagents may be explained by the formation of cross-links between organized structures in the case of glutaraldehyde. Apparently the cross-linking of F_2a_1 tetramers resulted in the formation of high molecular weight material.

Similar results were obtained with other histones. F_2a_2 (Figure 3D) and F_2b (Figure 3E) at a concentration of 1.0 mg/ml when cross-linked for 1 hr exhibited in addition to a high molecular weight components bands running from monomer to hexamer. When cross-linked for 16 hr most of the material present in F_2b was on top of the gel (broken line, Figure 3E). Apparently the cross-linking reaction shifted the equilibrium toward the high molecular weight fraction.

The results presented so far indicate that each of the acid-extracted and purified histone fractions can renature and reversibly self-assemble into high molecular weight structures. The fact that histones can aggregate to form high molecular weight structures has been observed by others before. Ziccardi and Shumaker (1973) have noted that the $s_{20,w}$ of histone F_2a_1 changes from 0.6 S in 5 mM NaCl to 19.2 S in 0.1 M NaCl. Boublik et al. (1970a) correlated the change in proton resonance spectra of F_2a_1, upon rais-

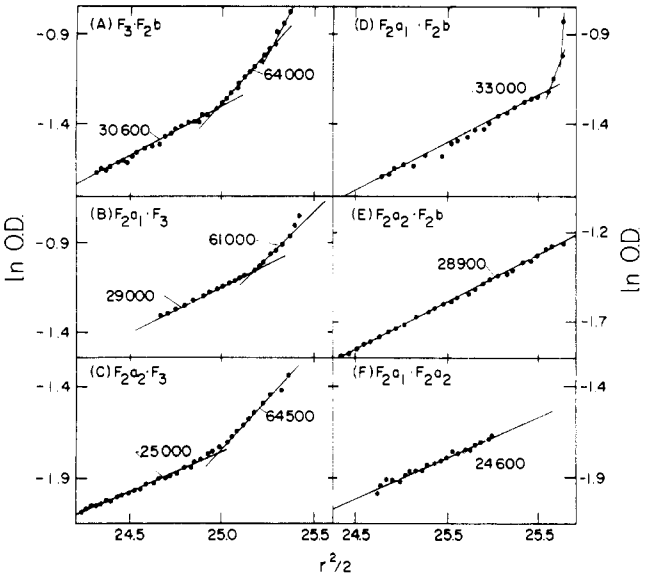

FIGURE 4: Sedimentation equilibrium of histone pairs. Histone pairs at 1.0 mg/ml of protein, $I = 0.15$, 5°, were subjected to sedimentation equilibrium runs as described under Materials and Methods. For the calculation of molecular weights a value of 0.74 $cm^3\ g^{-1}$ was used for $\bar{V}$. (A) F_3·F_2b; (B) F_2a_1·F_3; (C) F_2a_2·F_3; (D) F_2a_1·F_2b; (E) F_2a_2·F_2b; (F) F_2a_1·F_2a_2.

ing the ionic strength, with specific aggregation involving the carboxyl terminal of the molecule. Wickett et al. (1972) reported that the changes in the circular dichroism spectrum of histone F_2a_1 upon addition of salt indicate aggregation and β-sheet formation. This aggregation is highly dependent on temperature (Smerdon and Isenberg, 1973).

Similar results of aggregation were reported for F_2b: Boublik et al. (1970b) reported that this histone undergoes salt induced interchain interactions. On the other hand, D'Anna and Isenberg (1972) failed to observe aggregation upon addition of salt to F_2b; however, they worked at very low protein concentrations. Edwards and Shooter (1969) studied the molecular weight of this histone and noted a progressive aggregation as the salt concentration increased.

The conformation of F_2a_2 (D'Anna and Isenberg, 1974a; Bradbury et al., 1973) is also dependent on ionic strength. D'Anna and Isenberg (1974a) have noted that histone F_2a_2 shows a slow increase in anisotropy suggesting a slow aggregation.

The conformational changes occurring in F_3 as a function of salt concentration have been studied by D'Anna and Isenberg (1974e). They found these changes to be similar to those occurring in F_2a_1. First a fast step occurs which involves α-helix formation. This step is followed by a slow aggregation.

In summary our results are in agreement with the data obtained by others. These data indicate that under appropriate conditions single histone species aggregate into large molecular weight components. We wish to emphasize that this aggregation represents an ordered process of self-assembly. We have shown previously that F_2a_1 can reversibly self-assemble into well-defined periodic structures observed by the electron microscope (Sperling and Bustin, 1974). In this manuscript we present evidence that histones F_3, F_2b, and F_2a_2 can also self-assemble to form very similar structures to those obtained by F_2a_1. Thus for every histone the same structures will be obtained but under different experimental conditions.

II. Pairs of Histones

Several reports appeared which indicate that pairs of histones complex into dimers and tetramers. On the other hand, single histones assemble to give high molecular weight structures.

It could therefore be argued that lack of formation of high molecular weight structures, upon mixing pairs of histones, is an indication of interaction between these histones. This was the approach taken by us to follow interaction between pairs of histones in the six possible combinations formed from F_2a_1, F_3, F_2a_2, and F_2b.

F_2a_1·F_2b. Sedimentation velocity measurements (Figure 1) indicated that this is an interacting pair. A single peak (95% of material) with an $s_{20,w}$ of 2.8 S was observed. Sedimentation at 20° did not alter the percentage of the low molecular weight peak. However, this low molecular weight complex was found to be in equilibrium with a high molecular weight fraction whose percentage increased upon raising the ionic strength and protein concentration. Thus, raising the ionic strength to $I = 0.3$ (at 5°) yielded 20% of a 17S fraction and 80% of a 2.6S fraction. Similar shift of the equilibrium to higher molecular weight forms is observed when the protein concentration is raised to 3.0 mg/ml. At this protein concentration, $I = 0.15$ at 5°, 20% of the material sedimented with an $s_{20,w}$ of about 17 S. The molecular weight obtained by sedimentation equilibrium was 33,000 (Figure 4D). The calculated molecular weight of the dimer is 25,000, therefore, the sedimentation equilibrium results suggest the presence of both a dimer and higher molecular weight species. Indeed the results obtained from electrophoresis of the cross-linked pair on polyacrylamide gels revealed in addition to the monomers the presence of a band with a molecular weight of 25,000 and a band with a molecular weight of 50,000 (Figure 5C). The quantitative ratios of the two bands was 2:1, respectively. Neither of these bands was present when the parent species were cross-linked and analyzed under the same conditions. Examination of the solution with the electron microscope at $I = 0.15$ failed to reveal the presence of organized structures. These results are obtained when the parent histones were first mixed at low ionic strength and later dialyzed to higher ionic strength ($I = 0.15$). However, when the single histones are mixed directly at $I = 0.15$ we have observed that the relative amount of the high molecular weight component significantly increases, as detected by acrylamide gels and by electron microscopy. When the ionic strength was raised to 0.3 assembly into organized structures was observed (Figure 7A). Increase to $I = 0.5$ or change of buffer to phosphate leads to formation of longer fibers. Thus, a pair of strongly interacting histones can assemble into large structures.

D'Anna and Isenberg (1974) have reported that F_2a_1 and F_2b interact in a 1:1 ratio with a binding constant of 10^5–$10^6\ M^{-1}$. Our sedimentation velocity measurements show that this is an interacting system which forms a low molecular weight complex. The sedimentation equilibrium and acrylamide gel electrophoresis of the cross-linked complex show that this complex is mostly a heterodimer in equilibrium with a heterotetramer. However, the low molecular weight complexes are in equilibrium with a higher molecular weight fraction. The equilibrium is shifted toward this fraction by increase of protein concentration and ionic strength.

F_2a_1·F_3. Sedimentation velocity measurements of this

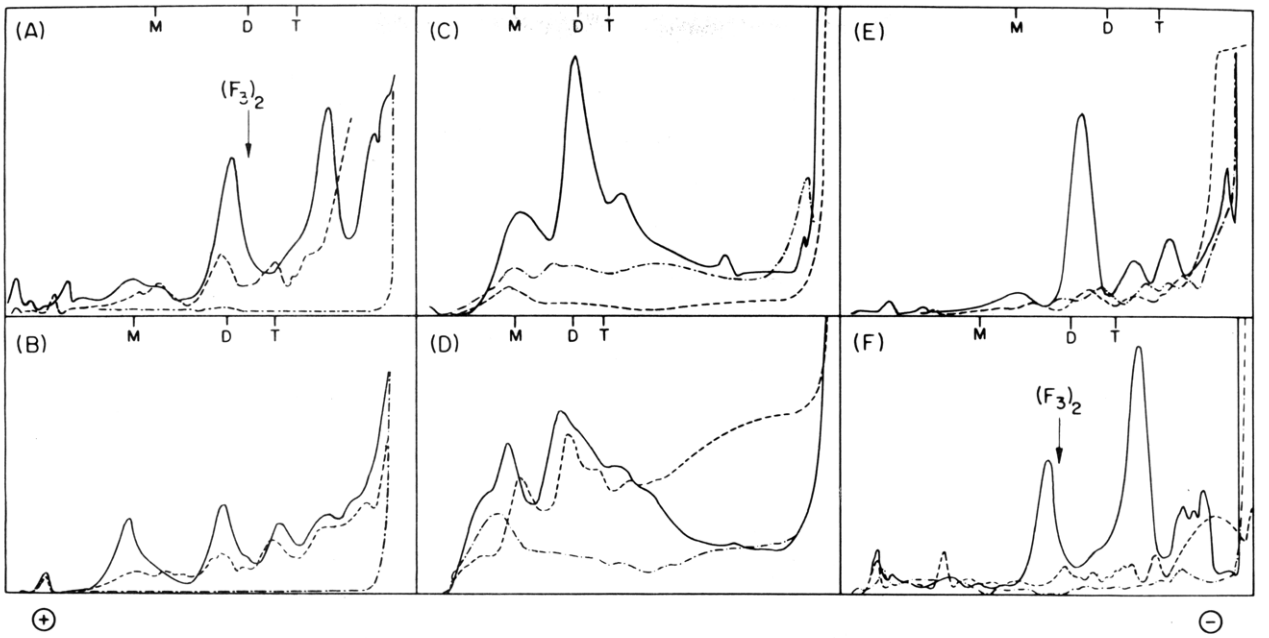

FIGURE 5: Electrophoresis of cross-linked histones pairs on 0.1% sodium dodecyl sulfate containing gels. Histones at $I = 0.15$, 5°, were cross-linked with dimethyl suberimidate as described under Materials and Methods. (A) F_3·F_2b (—), F_3 (- · -), F_2b (- - -); (B) F_3·F_2a_2 (—), F_3 (- · -), F_2a_2 (- - -); (C) F_2a_1·F_2b (—), F_2a_1 (- - -), F_2b (- · -); (D) F_2a_1·F_2a_2 (—), F_2a_1 (- · -); F_2a_2 (- - -); (E) F_2a_2·F_2b (—), F_2a_2 (- · -), F_2b (- - -); (F) F_2a_1·F_3 (—), F_2a_1 (- · -), F_3 (- - -). $(F_3)_2$ denotes position of dimer. M, D, and T denote the position of F_3 monomer, dimer, and trimer, respectively. A, B, E, and F, protein concentration 2 mg/ml for the pair, 1 mg/ml for the single histones, cross-linked for 1 hr, run on 10% gels. C and D, protein concentration 1 mg/ml for the pair, 0.5 mg/ml for the single histones, cross-linked for 4 hr, run on 4% gels.

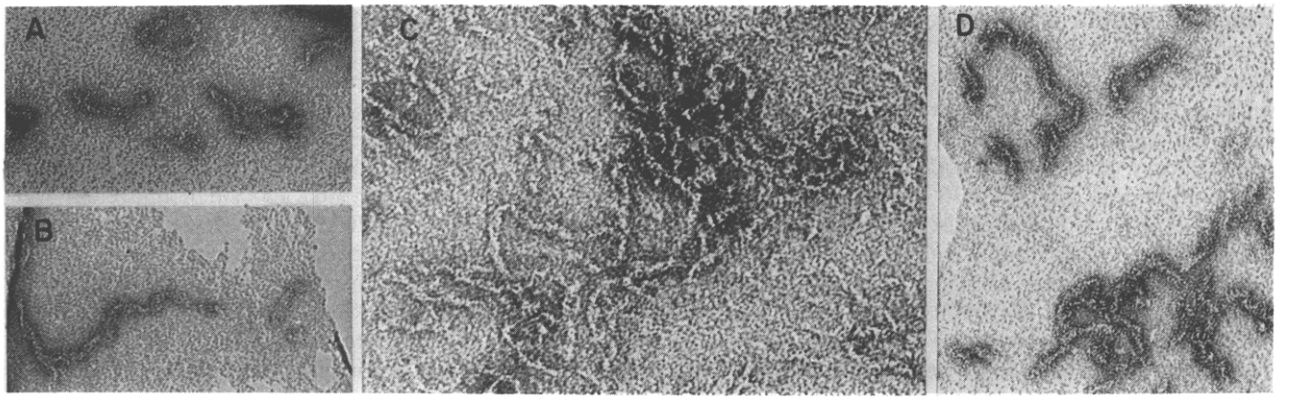

FIGURE 6: Assembly of F_3·F_2a_1 histone pair into organized structures. Electron micrographs of histone solutions at 2.0 mg/ml protein. (A) $I = 0.15$, ×140,000; (B) $I = 0.3$, ×150,000; (C) $I = 0.5$, ×150,000; A–C in cacodylate buffer. (D) $I = 0.15$, phosphate buffer, ×140,000. (B) and (D) were photographed over holes in the carbon-coated grids.

histone pair at concentration of 2.0 mg/ml of protein, $I = 0.15$ at 5°, show two fractions (Figure 1): one with an $s_{20,w}$ 2.6 and the other with $s_{20,w}$ 20.0. The two fractions were present in approximately equal amounts (Figure 1). The relative proportion of the two peaks was highly dependent on protein concentration. At 3.0 mg/ml of protein the proportion of the high molecular weight peak increased to 65% while at 0.70 mg/ml of protein it decreased to 20%. These findings strongly support the concept of a dynamic equilibrium between the high and low molecular weight component of this pair. This equilibrium is temperature dependent, as at 20° in a solution containing 2.0 mg/ml of total protein, the percentage of the high molecular weight fraction was 80%. This equilibrium is also ionic strength dependent as at $I = 0.3$, 5° (2 mg/ml), the percentage of the high molecular weight fraction increased to over 70%. Sedimentation equilibrium studies (at speeds which would sediment the high molecular weight fraction to the bottom of the cell) revealed the presence of a dimer with a molecular weight of 29,000 and a tetramer with a molecular weight of 61,000 (Figure 4B). From this curve we have estimated an association constant of 5×10^4 l./mol for a dimer–tetramer equilibrium.

A comparison of the gel electrophoretic pattern of the cross-linked mixed histones to that of the cross-linked parent species (see Figure 5F) also revealed the presence of a *mixed* dimer and *mixed* tetramer in a ratio of 1:2 and of higher molecular weight species. In the parent species only high molecular weight material was present.

Electron micrographs of this pair demonstrate the strong influence of environmental condition on the assembly of this strongly interacting pair into high molecular weight, organized structures. Thus at $I = 0.15$ bent rods with diameter of 22–44 Å can be observed (Figure 6A). At $I = 0.3$ these bent rods assemble into intertwined fibers (Figure 6B). At $I = 0.5$ the whole grid is covered with long intertwined fibers

(Figure 6C). In 5 m*M* phosphate buffer long intertwined fibers can be seen at $I = 0.15$ (Figure 6D). Clearly this pair of histones assembles into organized, large structures.

To summarize, our results indicate that this is an interacting pair of histones. At low protein concentration the major fraction is an assembled heterotetramer accompanied by a fraction of a heterodimer and fractions of high molecular weight. These fractions are in equilibrium, which is affected by: (1) protein concentration, (2) ionic strength, and (3) temperature. An increase in any of these parameters shifts the equilibrium toward the higher molecular weight fractions.

$F_2a_1 \cdot F_3$ complexes have been isolated by extracting chromatin with salt according to van der Westhuyzen and von Holt (1971). Kornberg and Thomas (1974) reported that the only species present is the tetramer. On the basis of equilibrium sedimentation Roark et al. (1974) found that the complex formed by these histones is a dimer which is in a concentration dependent equilibrium with a tetramer. D'Anna and Isenberg (1974c) reported that these proteins interact at a 1:1 molar ratio with a binding constant of $0.7 \times 10^{21}\ M^{-3}$. This tetramer can be formed from renatured histones at low protein concentrations. At protein concentrations higher than 0.65 mg/ml some of the renatured material has a high molecular weight (D'Anna and Isenberg, 1974d). It seems therefore that both our results and those reported by others can be explained by assuming a dynamic equilibrium between the various interacting species.

$F_2a_2 \cdot F_2b$. Sedimentation velocity measurements (Figure 1) indicated that this is an interacting pair. A single peak with an $s_{20,w}$ of 2.3 was observed. Upon raising the protein concentration to 3.0 mg/ml, 10% of the material sedimented with an $s_{20,w}$ of 15 S. An increase in ionic strength to $I = 0.3$ at 2.0 mg/ml of protein shifted the equilibrium to increase the heavy component. Under these conditions 70% of the material had an $s_{20,w}$ of 2.35 and 30% of the material had an $s_{20,w}$ of 15 S. The effect of temperature on this pair was negligible. Sedimentation equilibrium studies at $I = 0.15$ revealed the presence of a homogeneous dimer species with a molecular weight of 28,900 (Figure 4E). On polyacrylamide gels the cross-linked pair exhibited a major band corresponding to the molecular weight of the mixed dimer (Figure 5E). This band was absent in the cross-linked parent histones.

Examination by the electron microscope at $I = 0.15$ failed to show the presence of high molecular weight organized structure. However, in this pair bent rods become visible when the ionic strength was raised to $I = 0.5$.

Kelley (1973) and Skandrani et al. (1972) reported the isolation of an $F_2a_2 \cdot F_2b$ dimer. Kornberg and Thomas (1974) reported that these two histones interact to form oligomers. D'Anna and Isenberg (1974b) reported a 1:1 complex of histone F_2a_2 and histone F_2b with a binding constant of $10^6\ M^{-1}$. They reported that these two histones form a dimer plus a high molecular weight aggregate. Our results show that renatured F_2a_2 and F_2b interact to form a dimer. This dimer, however, is in equilibrium with a high molecular weight fraction which is formed upon increase of protein concentration or ionic strength. The tendency to form a high molecular weight species is much less remarkable than that of the $F_2a_1 \cdot F_3$ pair.

$F_2a_1 \cdot F_2a_2$. Sedimentation velocity at 5° and 2.0 mg/ml of protein revealed the presence of a peak with an $s_{20,w}$ of 3.2 (65%) and a high molecular weight fraction with an $s_{20,w}$ of 19 S (35%) (see Figure 1). At 20° the proportion of the high molecular weight component increased to 50%. At $I = 0.3$ and 5°, the proportion of the high molecular weight component was 60%. Sedimentation equilibrium measurements at speeds which sediment the high molecular weight component revealed the presence of a component with a molecular weight of 24,600 (Figure 4F). Analysis of the cross-linked pair on polyacrylamide gels revealed the presence of monomers, a dimer, and a tetramer (see Figure 5D). The cross-linked F_2a_1 showed only high molecular weight bands. The cross-linked F_2a_2 showed bands with mobilities corresponding to species ranging from monomer to pentamer and a large portion of the material migrating as a very diffuse band with a molecular weight over 60,000. Comparison of the cross-linked F_2a_2 with the cross-linked pair $F_2a_1 \cdot F_2a_2$ (Figure 5D) indicated that this diffuse high molecular weight fraction is not present in the $F_2a_1 \cdot F_2a_2$ pair.

These results suggest that the two histones interact. It is possible that the low molecular weight component is composed of both hetero- and homodimers and tetramers. Examination by electron microscopy revealed the presence of bent rods similar to those observed with F_2a_1 alone. These rods become more prominent at $I = 0.3$ (Figure 7B). A change of buffer to 5 m*M* phosphate, $I = 0.15$ (NaCl), leads to a striking assembly (Figure 7C). The possibility that these two histones interact has been raised by D'Anna and Isenberg (1974b). These authors found that the proteins form an equimolar complex with a low association constant of $4 \times 10^4\ M^{-1}$. Recently, based on evidence obtained by ^{13}C nuclear magnetic resonance studies, Clark et al. (1974) conclude that histones F_2a_1 and F_2a_2 interact.

Our results also suggest that these histones interact. However, since this interaction is weak, it is impossible at the present state to say whether the assembled fibers are of single histones, of mixed histones, or of both.

$F_3 \cdot F_2a_2$. Sedimentation velocity (Figure 1) revealed the presence of two components. The small molecular weight component comprising 70% of the material had an $s_{20,w}$ of 2.7 S; the rest of the material had an $s_{20,w}$ of 14 S. At 20° the relative amounts of the high molecular weight components increased to 40%. Sedimentation equilibrium (Figure 4C) revealed the presence of a dimer (mol wt 25,000) and a tetramer (64,500). From this figure we have estimated an association constant of 4×10^4 l./mol for a dimer-tetramer equilibrium. On polyacrylamide gels (Figure 5B) the cross-linked pair exhibited monomers, dimers, trimers, and tetramers together with high molecular weight species. However, none of the bands were prominent and the pattern did not differ much from that of the cross-linked parent histones. Therefore the cross-linking data do not allow us to determine whether this is an interacting pair. In the electron microscope bent rods were observed. These could result from F_3 self-assembly. D'Anna and Isenberg (1974c) noted interaction between this pair of histones. Our results show that F_3 and F_2a_2 interact as addition of F_2a_2 interferes with the self-assembly of F_3. However, the binding constant is probably low and a mixture of hetero- and homodimers and tetramers is probably present.

$F_3 \cdot F_2b$. Sedimentation velocity (Figure 1) revealed the presence of two species. The low molecular weight species comprising 70% of the material had an $s_{20,w}$ of 1.7 S; the rest of the material sedimented as a broad peak with an $s_{20,w}$ of 7.9 S. At 20° the proportion of the high molecular weight component increased to 50%.

Sedimentation equilibrium studies (Figure 4A) revealed the presence of a dimer and a tetramer species. From these

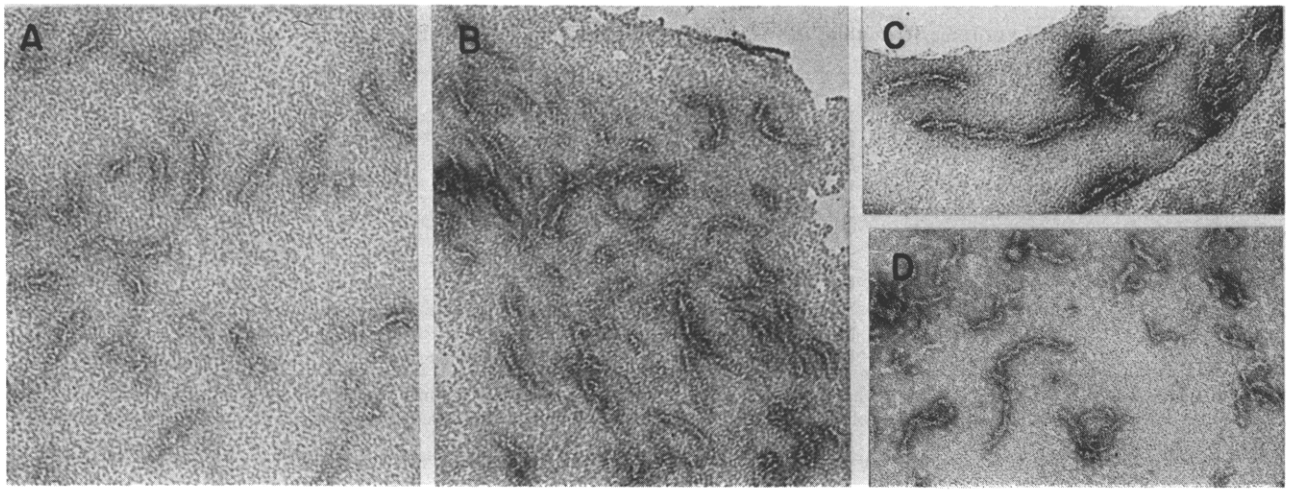

FIGURE 7: Assembly of histone pairs into organized structures. (A) $F_2a_1 \cdot F_2b$, $I = 0.3$, ×180,000; (B) $F_2a_1 \cdot F_2a_2$, $I = 0.3$, ×180,000; (C and D) $F_2a_1 \cdot F_2a_2$, $I = 0.15$, phosphate buffer; C, ×168,000 D, ×110,000. A, B, and C were photographed over holes in the carbon-coated grid. Protein concentration, 2.0 mg/ml. A and B in cacodylate buffer.

Table II: Reversibility of Fiber Formation in the Assembly of Histone Pairs.[a]

	$I = 0.5$			$I = 0.3$			$I = 0.15$			$I = 0.05$		
Histone Pair	L	H	Structure Observed by EM	L	H	Structure observed by EM	L	H	Structure observed by EM	L	H	Structure observed by EM
$F_2a_1 \cdot F_2b$	2.6 S 60%	17 S 40%	Rods and fibers	2.6 S (30%)	17 S (20%)	Rods	2.4 S (95%)		–	1.9 S (100%)		–
$F_2a_1 \cdot F_2a_2$				2.4 S (40%)	19 S (60%)	Fibers	2.3 S (65%)	18 S (35%)	Rods	1.8 S (95%)		–
$F_2a_1 \cdot F_3$				2.6 S (25%)	21 S (75%)	Fibers	1.9 S (35%)	21 S (65%)	Rods	1.9 S (50%)	19 S (50%)	Rods

[a] Results obtained when histone pairs were back dialyzed from high to low ionic strength. Histone pairs at 2.0 mg/ml, 5°, solutions buffered to pH 7.0 with sodium cacodylate ($I = 0.01$), were first gradually dialyzed to $I = 0.3$ (all ionic strengths were adjusted with NaCl). $F_2a_1 \cdot F_2b$ was further dialyzed to $I = 0.5$. After examination the solutions were back dialyzed to lower ionic strengths as indicated. The $s_{20,w}$ value and percentage of the slow sedimenting component (indicated in the table as L) and of the fast sedimenting component (H) are indicated. The presence or absence of fibers and rods observed by electron microscopy, at each ionic strength, is indicated. (–) No structure observed by EM (electron microscope).

data we have estimated an association constant of 4×10^4 mol/l. for the dimer–tetramer equilibrium. Analysis of this cross-linked pair on polyacrylamide gels (Figure 5A) indicates that these are mixed dimers and tetramers not observed in the analysis of the cross-linked parent histones. The ratio of dimer to tetramer was about 1:1. In the electron microscope a small amount of bent rods was observed. Interactions between this pair of histones have not been reported. D'Anna and Isenberg (1974c) postulate that if there is an interaction between these histones it is weak.

Our results indicate that this is an interacting pair forming a low molecular weight fraction which is composed of heterodimer and tetramer and this fraction is in equilibrium with a high molecular weight fraction whose formation is favored by increase in protein concentration, ionic strength, and temperature. However, since the strength of interaction between the two members of the pair is not known, it is possible that the high molecular weight components are either homo- or heteroaggregates, or a mixture of both.

Reversibility of Fiber Formation in the Assembly of Histone Pairs. To obtain further evidence that the assembly of histone pairs into organized fibers is indeed a reversible process, histone pairs prepared at low ionic strength have been gradually dialyzed to higher ionic strength and examined by sedimentation velocity and electron microscopy. When distinct fibers were observed the histone solutions were gradually dialyzed back to low ionic strength. The results obtained are summarized in Table II. It can be seen that in the histone pair $F_2a_1 \cdot F_2b$ the ionic strength had to be elevated to 0.5 for fiber formation. $F_2a_1 \cdot F_2b$ which have been dialyzed either to $I = 0.5$ or $I = 0.3$ gave the same results when back dialyzed to lower ionic strength. Histone pairs $F_2a_1 \cdot F_2a_2$ and $F_2a_1 \cdot F_3$ displayed a large amount of fibers already at $I = 0.3$, when back dialyzed to lower ionic strength histone pairs $F_2a_1 \cdot F_2a_2$ and $F_2a_1 \cdot F_3$ displayed rods at $I = 0.15$. The rods disintegrated at $I = 0.05$ in the case of histone pair $F_2a_1 \cdot F_2a_2$. We have previously reported (Sperling and Bustin, 1974) that the assembly of F_2a_1 is fully reversible. The data presented in Table II indicated that the structures which are formed in solutions which contain histone pairs can be reversibly dissociated.

Concluding Remarks

Table III summarizes the various assembled histone structures that can be obtained by varying the ionic strength. The data pertain to solutions at 5°, buffered with

Table III: Summary of the Effect of Ionic Strength of the Assembly of Histones and Histone Pairs.[a]

Histone	$I = 0.02$	$I = 0.15$	$I = 0.3$	$I = 0.5$
F_2a_1	No structure	Rods	Fibers	Fibers
F_3	Rods	Rods	Fibers	Fibers
F_2b	No structure	Very few rods	Rods	Fibers
F_2a_2	No structure	No structure	Very few rods	Rods
$F_2a_1 \cdot F_3$	No structure	Very few rods	Fibers	Fibers
$F_2a_1 \cdot F_2b$	No structure	No structure	Rods	Rods and fibers
$F_2a_1 \cdot F_2a_2$	No structure	Very few rods	Fibers	Fibers
$F_2b \cdot F_2a_2$	No structure	No structure	No structure	Few rods
$F_2b \cdot F_3$	No structure	No structure	Rods	Fibers
$F_2a_2 \cdot F_3$	No structure	Rods and some fibers	Rods and some fibers	Few rods many fibers

[a] Data for histones at 2.0 mg/ml, 5°, solutions buffered to pH 7.0 with sodium cacodylate, ionic strength, 0.01. Rods refer to the bent rods. Fibers are intertwined long fibers. No structure refers to the fact that no structures were observed by the electron microscope. These forms are described in the text.

sodium cacodylate, $I = 0.01$, pH 7.0, protein concentration, 2.0 mg/ml. Changes in temperature, type of buffer, or protein concentration will shift the equilibrium.

The results presented by us provide information on the pattern of histone assembly. The four histones F_2a_1, F_3, F_2a_2, and F_2b can be divided into two groups. One group, the arginine-rich histones F_2a_1 and F_3, have a strong tendency to self-assemble and form bent rods and intertwined fibers. These two histones also interact with each other strongly to give heterodimers, heterotetramers, and higher molecular weight structures. At high ionic strength or in phosphate buffer, we have observed long intertwined fibers with a diameter of 44 Å. The various structures are in a reversible equilibrium so that the final structure obtained is dependent on the protein concentration, ionic strength, and temperature.

The second group is the slightly lysine rich histones F_2b and F_2a_2. They require a higher ionic strength for self-assembly into large structures. These two histones strongly interact with each other. There are also pairwise cross-interactions between members of the arginine and of the lysine-rich group. Furthermore, each pair under certain ionic strength can assemble into organized structures observable by the electron microscope. At high ionic strengths (I = 0.3–0.5) an intertwined histone fiber structure was obtained. We are presently investigating whether the fibers obtained from pairs of histones are homo- or heterofibers. As the assembly of histones is dependent on several parameters the structure observed at high ionic strength can also be obtained at physiological ionic strengths ($I = 0.15$) when the buffer was changed to phosphate. In the cell nucleus the histones assemble in the presence of DNA which may influence this assembly. Currently we are studying the influence of DNA on the assembly process of histones.

The self-interaction of purified histones reported represents a reversible ordered process of self-assembly of renatured histones. However, as with other proteins (Anfinsen, 1973) for proper renaturation it is necessary to first dissolve the histones at low ionic strength. The conditions which promote assembly vary little from histone to histone. The dimensions and the shape of the assembled structures are very similar among the histones. In each case the first structure observed is a bent rod with a diameter of about 22 Å. Conditions which favor assembly lead to formation of intertwined fibers with diameters of about 44 Å. We have suggested that in chromatin DNA may be wrapped around assembled F_2a_1 structures, or F_2a_1 like histone structures (Sperling and Bustin, 1974). If this can happen, then the results presented here suggest that each of the histones by themselves or in pairs can form structures around which the DNA can be wrapped. Indeed it has been noted that each of the histones interact with DNA in a cooperative fashion (Akinrimisi et al., 1965).

Since the histones assemble into similar structures it is also possible that they can replace one another. Indeed Gorowsky (1973) reported that the amount of histone F_3 in the micronuclei of tetrahymena is greatly reduced. As F_2a_1 is very similar to F_3 in its structural behavior it can probably substitute F_3 in this organism.

Once the histones have assembled and the structure stabilized by interaction with DNA it is unlikely that they will reorganize. Indeed Tsanev and Russev (1974) showed that histones do not redistribute during cell replication. However, the composition of the histone subunit in chromatin is still an open question and it probably depends on the exact conditions which prevail in the nucleus during chromatin assembly.

The question rises whether the bent rod or intertwined fiber structure can be present in the "native" chromatin fiber. Olins and Olins (1974) have observed that the chromatin fiber is composed of repeating spherical bodies with a diameter of about 80 Å. Kornberg (1974) proposed that the structure of the repeating unit of chromatin is composed of 200 base pairs of DNA complexed with two of each of the histones F_2a_1, F_3, F_2b, and F_2a_2. If the basic histone structure observed by us, i.e., the "bent rod" is an octamer, around which the DNA is wrapped, then each chromatin bead may contain a bent rod of histones. The size of such a unit could fit the reported dimensions of the ν bodies. As all histones form similar structures, the histone composition in each bead may vary. As there is an equilibrium between the bent rod and the intertwined fiber structure we suggest that a transition between these two forms in the histone core may serve as a mechanism for reversible condensation of chromatin.

Acknowledgment

We are grateful to Dr. I. Z. Steinberg for helpful discussions and suggestions. We thank Dr. M. Hirschfeld for the equilibrium sedimentation runs, and Mrs. H. Kuppfer and Mrs. R. August for skillful help.

References

Akinrimisi, E. O., Bonner, J., and Ts'o, P. O. P. (1965), *J. Mol. Biol. 11*, 128–136.

Anfinsen, C. B. (1973), *Science 181,* 223–230.
Bohm, E. L., Strickland, W. N., Strickland, M., Thwaits, B. M., van der Westhuyzen, D. R., and von Holt, C. (1973), *FEBS Lett. 34,* 217–221.
Boublik, M., Bradbury, E. M., and Crane-Robinson, C. (1970a), *Eur. J. Biochem. 14,* 486–497.
Boublik, M., Bradbury, E. M., Crane-Robinson, C., and Johns, E. W. (1970b), *Eur. J. Biochem. 17,* 151–159.
Bradbury, E. M., Cary, P. D., Crane-Robinson, C., and Rattle, H. W. E. (1973), *Ann. N.Y. Acad. Sci. 222,* 266–288.
Clark, V. M., Lilley, D. M. J., Howarth, O. W., Richards, B. M., and Pardon, J. F. (1974), *Nucleic Acid Res. 1,* 865–880.
D'Anna, J. A., and Isenberg, I. (1972), *Biochemistry 11,* 4017–4025.
D'Anna, J. A., and Isenberg, I. (1973), *Biochemistry 12,* 1035–1043.
D'Anna, J. A., and Isenberg, I. (1974a), *Biochemistry 13,* 2093–2098.
D'Anna, J. A., and Isenberg, I. (1974b), *Biochemistry 13,* 2098–2104.
D'Anna, J. A., and Isenberg, I. (1974c), *Biochemistry 13,* 4992–4997.
D'Anna, J. A., and Isenberg, I. (1974d), *Biochem. Biophys. Res. Commun. 61,* 343–347.
D'Anna, J. A., and Isenberg, I. (1974e), *Biochemistry 13,* 4987–4992.
Davies, G. E., and Stark, G. R. (1970), *Proc. Natl. Acad. Sci. U.S.A. 66,* 651–656.
Edwards, P. A., and Shooter, K. V. (1969), *Biochem. J. 114,* 227–235.
Gorowsky, N. A. (1973), *J. Protozool. 20,* 19–25.
Hnilica, L. S. (1972), The Structure and Biological Function of Histones, Cleveland, Ohio, Chemical Rubber Publishing Co.
Johns, E. W. (1971), in Histones and Nucleohistones, Phillips, D. M. P., Ed., New York, N.Y., Plenum Publishing Co., p 37.
Kelley, R. I. (1973), *Biochem. Biophys. Res. Commun. 54,* 1588–1594.
Kornberg, R. D. (1974), *Science 184,* 868–871.
Kornberg, R. D., and Thomas, J. O. (1974), *Science 184,* 865–868.
Li, H. J., Wickett, R. R., Craig, A. M., and Isenberg, I. (1972), *Biopolymers 11,* 375–397.
Luck, J. M., Rasmussen, P. S., Satake, K., and Tsvertikov, A. N. (1958), *J. Biol. Chem. 233,* 1407–1414.
Olins, A. L., and Olins, D. E. (1974), *Science 183,* 330–332.
Panyim, S., and Chalkley, R. (1969), *Arch. Biochem. Biophys. 130,* 337–346.
Roark, D. E., Geoghezan, T. E., and Keller, G. H. (1974), *Biochem. Biophys. Res. Commun. 59,* 542–547.
Ruiz-Carrillo, A., and Allfrey, V. G. (1973), *Arch. Biochem. Biophys. 154,* 185–191.
Skandrani, E., Mizon, J., Santiere, P., and Biserte, G. (1972), *Biochimie 54,* 1267–1272.
Smerdon, M. J., and Isenberg, I. (1973), *Biochem. Biophys. Res. Commun. 55,* 1029–1034.
Sperling, R., and Bustin, M. (1974), *Proc. Natl. Acad. Sci. U.S.A. 71,* 4265–4269.
Tsanev, R., and Russev, G. (1974), *Eur. J. Biochem. 42,* 257–263.
van der Westhuyzen, D. R., and von Holt, C. (1971), *FEBS Lett. 14,* 333–337.
Varshavsky, A. J., and Georgiev, G. P. (1972), *Biochim. Biophys. Acta 281,* 669–674.
Weber, K., and Osborn, M. (1969), *J. Biol. Chem. 244,* 4406–4412.
Wickett, R. R., Li, H. J., and Isenberg, I. (1972), *Biochemistry 11,* 2952–2957.
Ziccardi, R., and Shumaker, V. (1973), *Biochemistry 12,* 3231–3235.